

## Hardness optimization of boride diffusion layer on ASTM F-75 alloy using response surface methodology

J.L. Arguelles-Ojeda<sup>a,b</sup>, A. Márquez-Herrera<sup>c,\*</sup>, A.L. Saldaña-Robles<sup>c</sup>, A. Saldaña-Robles<sup>c</sup>,  
M.A. Corona-Rivera<sup>a,d</sup>, and J. Moreno-Palmerin<sup>e</sup>

<sup>a</sup>*Doctorado Institucional en Ingeniería y Ciencia de Materiales,  
Universidad Autónoma de San Luis Potosí, San Luis Potosí, SLP 78000, México.*

<sup>b</sup>*Ingeniería Mecánica Administrativa, COARA,  
Universidad Autónoma de San Luis Potosí, Matehuala, SLP 78700, México.*

<sup>c</sup>*Ingeniería Mecánica Agrícola, DICIVA,  
Universidad de Guanajuato, Irapuato, Guanajuato 36500, México.*

\**e-mail: amarquez@ugto.mx*

<sup>d</sup>*Ingeniería Química, COARA-Universidad Autónoma de San Luis Potosí,  
Matehuala, SLP 78700, México.*

<sup>e</sup>*Departamento de Minas, Metalurgia y Geología, Universidad de Guanajuato,  
Ex-Hacienda San Matías s/n, Guanajuato, Guanajuato, 36020, México.*

Received 25 July 2016; accepted 31 October 2016

In this study, the Response Surface Methodology (RSM) and Central Composite Design (CCD) were used to optimize the hardness of boride diffusion layer on ASTM F-75 alloy (also called Haynes alloy). A boronizing thermochemical treatment was carried out at different temperatures and for different time periods. Hardness tests were conducted. The boride diffusion layer was verified by the X-ray diffraction (XRD) analysis indicating the formation of CoB, Co<sub>2</sub>B, CrB and Mo<sub>2</sub>B phases. An optimal hardness of 3139.7 HV was obtained for the samples subjected to the boriding process for a duration of 6.86 h at 802.4°C.

**Keywords:** ASTM F-75; CoCrMo; boriding; RSM; haynes alloy.

PACS: 62.20.Dc; 62.20.Fe; 62.20.Mk

### 1. Introduction

At present, ASTM F-75 alloy (CoCrMo) is one of the most important alloys used for orthopedics applications. This alloy is characterized by a superior wear and corrosion resistance and a high level of hardness. Therefore, it is the metal of choice for articulating the surface of joint hip and knee replacements [1]. Despite numerous applications in orthopedics, which are partly based on its corrosion resistance, this alloy has a long history in aerospace and gas turbine industries which exploit its hardness as an important mechanical property [2]. The use of surface coatings offers a possibility to design materials having required properties for a special demand.

Several technologies are currently used in the industries for the surface hardening of steels, ferrous or non-ferrous alloys, and some super alloys [3]. In addition to the high level demand in the improvement of surface hardening, it is also extremely important to improve the industrial processes by increasing the resistance of materials against wear [4]. With the emergence of high-speed processing technology, this issue has become very relevant [4,5]. Therefore, the modern hardening techniques are expected to gratify these requirements. The improvement in hardness can be obtained via coating or diffusion penetration on the metal by a process such as nitriding, carburization, carbonitriding, physical vapour deposition (PVD) method, chemi-

cal vapour deposition (CVD) method etc. [5-9]. Although, these treatments improve wear performance, coating techniques have adhesion problems, while diffusion penetration as thermochemical treatments have excellent adhesion bonding between diffusion layer and substrate but they are expensive and require complex equipment. In recent years, the boronizing (also called boriding) process has emerged as an alternative [4,10-23], and now accepted as an excellent choice for surface hardening. This process takes the advantage of the phenomenon of diffusion of boron into the metal surface to create the boride diffusion layer by heat treatment. The final boronized metal surface shows improvement in its mechanical properties such as greater hardness, better wear resistance, and greater resistance to corrosion and oxidation [15,22]. Although there are several boronizing methods [16-21] and many formulations [11,24-30] to produce the boride layer, this study considered boronizing process by employing a boron commercial paste.

Although, there are several studies investigating the boride hardness surface using different conditions [11-30], none of them used RSM to investigate the optimal conditions in boride process [18,31-37]. RSM is an experimental methodology, which allows finding of the optimal conditions of a process in an experimental region that is delimited by the experimental range of each factor, for determining the optimal values for the factors and predict target response [38]. RSM reduces the number of experimental trials and helps in

interpretation by making feasible the analysis of a large number of factors and delineating their possible mutual interactions [39]. Therefore, a systematic study of this process using RSM is very useful, and served the main objective of this research. This work was focused on the study of the surface hardening of ASTM F-75 alloy using the boronizing paste technique by RSM.

## 2. Experimental procedure

The boronizing process was carried out by employing the commercial Durborid<sup>®</sup> boron paste (typical it consists of 5 wt% B<sub>4</sub>C powder diluted with 90 wt% SiC of refractory material and 5 wt% KBF<sub>4</sub> as a flux). For thermal treatments, an alumina crucible and a conventional Barnstead International muffle, model FB1415M, were used. The X-ray diffraction (XRD) measurements were performed with a Rigaku X'pert diffractometer using the Cu<sub>Kα</sub> line ( $\lambda_{K\alpha 1}=1.54056 \text{ \AA}$  and  $\lambda_{K\alpha 2}=1.54439 \text{ \AA}$ ) and the correspondence between the experimental diffraction peaks and those from the database was made using the Match! 3 phase identification software. Measurements were taken from 25° to 70° with increments of 0.05°. Hardness was measured using a micro Vickers hardness tester model SMVK-1000ZS. The experimental procedure was carried out in three stages: samples preparation, paste boriding process, and layer analysis.

### 2.1. Preparation of the samples

ASTM F-75 alloy (CoCrMo alloy) was used as a substrate (25.4 mm diameter × 4 mm thickness). The chemical composition of CoCrMo alloy has a balanced weight percentage cobalt, 28-weight percentage chromium, and 6-weight percentage molybdenum. All samples were mechanically polished using SiC sandpaper from 240 to 1200 and then diamond paste with a mesh size of 3200 (7.9 μm). In order to clean the surface, the samples were washed consecutively in an ultrasonic bath with methanol, acetone, and isopropanol, and finally with deionized water; the duration of each step was 5 min. After cleaning, the surface hardness was measured before starting the boronizing process.

### 2.2. The boronizing process by response surface methodology

RSM was applied for the boronizing process. This methodology was used to design and optimize the boronizing process by considering two factors: temperature and time, and constructing a prediction model for the Vickers hardness, HV (response variable). A factor is a variable that is investigated in an experiment to understand as it affects the response variable. The values assigned to each factor in the experimental design are called levels, these levels are codified (1.41, 1, 0, -1, -1.41) to facilitate the interpretations and calculations in experimental designs.

TABLE I. Coded levels of factors.

Independent variable	Factor	Coded levels				
		-1.41	-1	0	1	1.41
Temperature (°C)	T	658.57	700	800	900	941.42
Time (h)	t	5.58	6	7	8	8.41

A central composite design (CCD) was used in the RSM to develop the experimental design. The coded levels and their values of the boronizing process are shown in Table I. The experimental data was evaluated by the analysis of variance (ANOVA), using STATGRAPHIC software. The design was based on a 2<sup>2</sup> factorial design completely randomized with three replicas. The CCD experiment was performed with 30 experiments: 4 factorial points (3 replicates), 2 central points and 4 axial points (3 replicates).

Each specimen was placed inside a dry pressing die of 50.8 mm diameter, and then 70 g of the boron paste was spread on the surface to deposit a layer having a thickness of about 3 cm. In order to enhance the contact, a load of 16 kN was applied over the pressing die for 10 min. Finally, the sample was placed on an alumina crucible and inserted inside the preheated muffle at the desired temperature and time as mentioned in Table I. The high temperature, shown in Table I, is not only acceptable for the lab, but also it is well applicable for industrial processing, while the low temperature is enough to activate the diffusion in the material.

After the boronizing process, the residual paste left on the surface was cleaned by washing the samples in boiling water and then were brushed using a toothbrush. Finally, the samples were washed consecutively in the ultrasonic bath as mentioned earlier.

### 2.3. Analysis of layer

The hardness test was performed before and after the boronizing process as per the ASTM E384 standard. The measurements were carried out by applying a load of 9.81 N for 15 s. The phase structure of the optimal boride diffusion layer was analyzed by X-ray diffraction method (XRD). The boride layer was evaluated on the cross sections by optical microscope (Olympus BX60), the sample was prepared by conventional metallographic and etching using a solution of 3 % HNO<sub>3</sub>, 1 % HCl and 94 % C<sub>2</sub>H<sub>6</sub>O.

## 3. Results and discussion

The hardness of the material ASTM F-75 before boronizing was 387 ± 7 HV. The variance analysis (ANOVA) for HV was carried out after verifying that HV data come from a normal distribution (Table II). A p-value less than 0.050 indicated significance of the terms employed in the model. For this model, the quadratic effects of temperature and time are

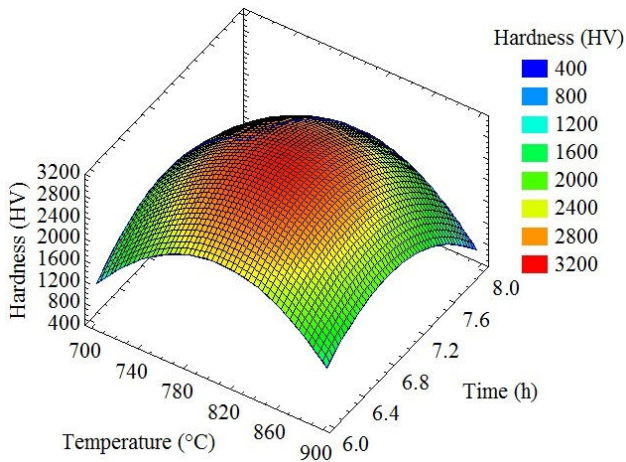


FIGURE 1. Estimate response surface for hardness (HV).

TABLE II. ANOVA for Hardness (HV).

VS	SS	DF	MS	F0	p-value
T: Temperature	13550.2	1	13550.2	0.14	0.7252
t: Time	450408	1	450408	4.73	0.0953
T <sup>2</sup>	6692870	1	6692870	70.26	0.0011
Tt	57104.3	1	57104.3	0.60	0.4820
t <sup>2</sup>	3369120	1	3369120	35.37	0.0040
Error	381039	4	95259.7		
Total	8242030	9			

VS = variability source; SS = sum of squares; DF = degrees of freedom; MS = mean square; F0 = test statistic; p-value = observed significance

less than 0.0040, indicating that the parameters have a significant effect on HV. The coefficient of determination ( $R^2$ ), for the model, is equal to 95.4 %, which indicates that the boronizing parameters explain 95.4 % of variance in HV.

A regression model was applied to the experimental data to predict the value of hardness (HV) at the different values of the factors employed. Temperature (T) and time (t) were used as the parameters to model HV. Eq. (1) is the regression equation for HV. This expression is applicable only within the experimental region; the magnitudes of the variables are specified in their original units.

$$HV = -121742 + 202.374 + 12737.4t - 0.120999T^2 - 1.19482Tt - 858.487t^2 \quad (1)$$

An analysis of the response surface and contour plots helped in optimizing the efficiency of HV. Fig. 1 shows the response surface for HV indicating the mean hardness value (HV) in the experimental region. The response surface of the HV increased with increasing the time from 6 h to 6.8 h however, when the time was increased from 6.8 h to 8 h, the HV decreased. Interestingly, a similar effect on the temperature was also observed; when the temperature was increased from 700°C to 780°C, the HV increased, but when the temperature

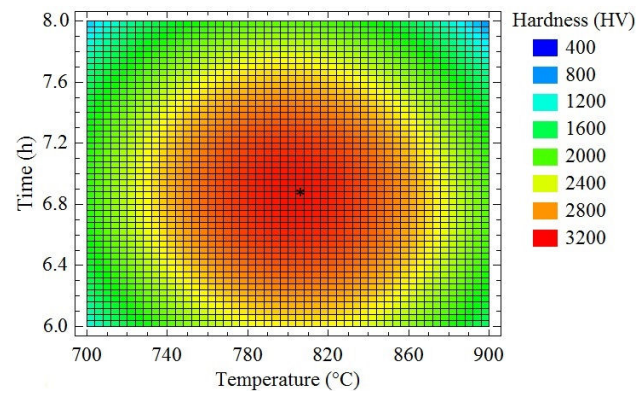


FIGURE 2. Contour of estimate response surface for Hardness (HV).

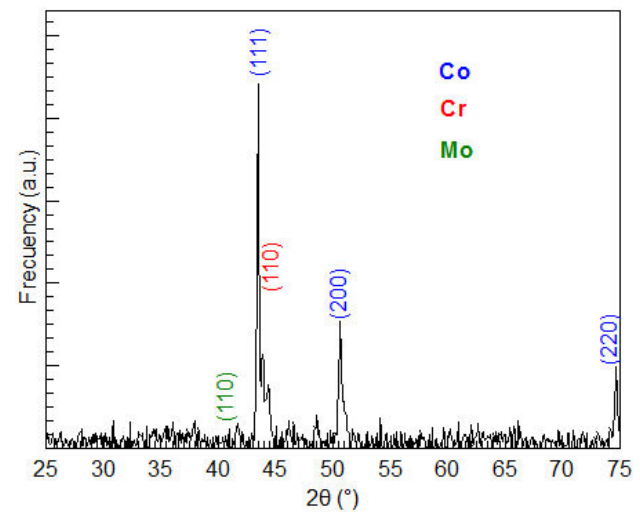


FIGURE 3. XRD pattern obtained at the surface of the ASTM F-75 cobalt alloy before boronizing.

was increased further from 780°C to 900°C, the HV decreased. The RSM enabled us to determine the optimal region and depict the optimal response; and it demonstrated the optimization of the boronizing process parameters for HV.

Figure 2 shows the contour of estimate response surface for hardness (HV). The optimal point for this model is shown in the figure. The levels that maximize 3139.7 HV (30.79 GPa) over the indicated region are a temperature of 802.4°C and duration of 6.86 h.

It is important to note that the optimal hardness estimated by RMS is higher than earlier published hardness results [18, 33, 34, 40-43]. Although the data obtained by these authors did not use the same indentation conditions (indentation load and time), the hardness can be properly compared since these authors use the same standard.

Figure 3 shows the X-ray diffractogram of the sample before boronizing. The positions of the diffraction peaks associated with the crystal structure of Co, Cr and Mo, obtained respectively from 150806, 60694 and 421120 card of the powder diffraction files (PDF) database, are also shown. The X-ray diffraction analysis confirms that the material is

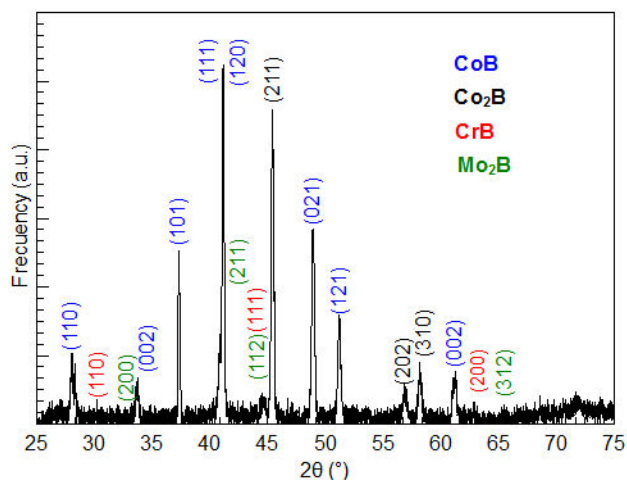


FIGURE 4. XRD pattern obtained at the surface of the boride ASTM F-75 cobalt alloy. The boronizing temperature was 800°C and the treatment duration was 7 h.

composed at least of Co and Cr because there is a complete correspondence between the diffraction peaks observed and those mentioned in database.

The samples prepared at 800°C and 7 h were in the best hardness conditions. In this sense, X-ray characterization of the samples prepared at this temperature and time was carried out. Figure 4 shows the X-ray diffractogram of the sample subjected to the optimum thermochemical hardening with boron. The positions of the diffraction peaks associated with the crystal structure of CoB, Co<sub>2</sub>B, CrB and Mo<sub>2</sub>B, obtained respectively from 30959, 250241, 320277 and 250561 card of the powder diffraction files (PDF) database, are also shown. The X-ray diffraction analysis confirms that the boride layer is composed of CoB, Co<sub>2</sub>B, CrB and Mo<sub>2</sub>B crystals, as there is a complete correspondence between the diffraction peaks observed and those mentioned in database. The strong and sharp diffraction peaks further affirm the crystalline nature of the layer.

The X-ray results suggest that the boron atoms diffuse into the material surface reacting with Co, Cr and Mo. It is assumed that the following reactions would take place si-

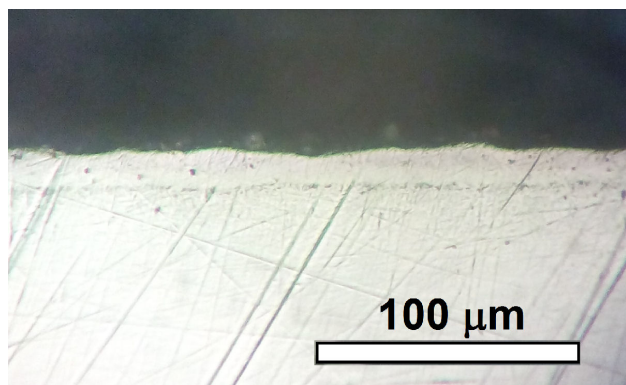


FIGURE 5. Optical micrograph of the cross-sectional microstructure of the boronized sample. The boronizing temperature was 800°C and the treatment duration was 7 h.

multaneously on the sample increasing the hardness of the boronized material on the surface:



During the annealing process, B<sub>4</sub>C becomes unstable and boron is liberated, and then it diffuses to interact with Co, Cr and Mo forming a boride layer which consists of complex borides mixture, Eq. (1-4). Since the Vickers hardness of CoB, Co<sub>2</sub>B, CrB and Mo<sub>2</sub>B phases have been measured as 30 Gpa [33], 17 GPa [33], 17 GPa [44] and 24.4 GPa [45], respectively, these phases are responsible for the increased hardness, which is probably the closest to the phase hardness value of greater volume fraction in the boride layer.

Figure 5 shows an optical micrograph of the cross-sectional microstructure of the boronized sample prepared at 800°C and 7 h. The obtained thickness of the boride layer is  $14.8 \pm 0.9 \mu\text{m}$ .

Even when the boronized layer is constituted by a mixture of phases as CoB, Co<sub>2</sub>B, CrB and Mo<sub>2</sub>B, at this resolution, the outer layer in Fig. 5 seems formed by one phase.

#### 4. Conclusions

In this study, the statistical design of the experiments and the RSM were found to be powerful tools for the planning and analysis of the experiments determining the influence of temperature and time of the boronizing process on the hardness of boride ASTM F-75 layers. The calculated regression models were found to be statistically significant at the required range and all experimental data fitted well with an R<sup>2</sup> value of 0.954.

A second-order polynomial response surface equation was developed in order to analyze the effect of variables on the layer hardness. The model shows that temperature has a significant effect, while time has no significant effect on the hardness. However, a proper combination of temperature and time of the boriding process can achieve a high level of hardness. The most optimal conditions, for the boriding process, were: temperature at 802.4°C and the duration of 6.86 h. Under this condition, the maximal hardness of 3129.7 HV was achieved.

Finally, the X-ray diffraction analysis confirmed that the boride layer of the best sample was composed of CoB, Co<sub>2</sub>B, CrB and Mo<sub>2</sub>B and the thickness of its boride layer is  $14.8 \pm 0.9 \mu\text{m}$ .

#### Acknowledgments

This work was supported by the Universidad de Guanajuato through project 525/2015.

1. J. Black, *Biological Performance of Materials: Fundamentals of Biocompatibility*, 4th ed., CRC Press, Boca Raton, (Florida, 2005).
2. D.J.S. Hyslop, A.M. Abdelkader, A. Cox, D.J. Fray, *Acta Materialia*, **58** (2010) 3124-3130. Doi: 10.1016/j.actamat.2010.01.053
3. L. Santo, J.P. Davim, *Surface Engineering Techniques and Applications: Research Advancements*, 1st Ed., IGI Global, (USA, 2014). Doi: 10.4018/978-1-4666-5141-8
4. T. Balusamy, T.S.N. Sankara-Narayanan, K. Ravichandran, I. Song-Park, M. Ho-Lee, *Vacuum*, **97** (2013) 36-43. Doi: 10.1016/j.vacuum.2013.04.006
5. J. Bedoya, N. Cinca, J.M. Guilemany, *Rev. Metal. Madrid*, **49** (2013) 223-236. Doi: 10.3989/revmetalm.1237
6. A.A. Amaya-Avila, O.E. Piamba-Tulcan, J.J. Olaya-Florez, *Ingeniería Mecánica Tecnología y Desarrollo* **5** (2015) 333-338.
7. L.F. Zagonel *et al.*, *Surface and Coatings Technology*, **207** (2012) 72-78. Doi: 10.1016/j.surfcoat.2012.05.081
8. K. Yagita, C. Ohki, *Plasma Nitriding Treatment of High Alloy Steel for Bearing Components*, *NTN Technical Review*, **78** (2010) 33-40.
9. S. Lampman, *Introduction to Surface Hardening of Steels, Heat Treating*, Vol. 4, (ASM Handbook, ASM International; 1991), pp. 259-267.
10. M. Kulka, N. Makuch, P. Dziarski, D. Mikoajczak, D. Przesacki, *Optics and Lasers in Engineering*, **67** (2015) 163-175. Doi: 10.1016/j.optlaseng.2014.11.015
11. I. Campos, M. Palomar-Pardavé, A. Amador, C. Villa-Velázquez, J. Hadad, *Appl. Surf. Sci* **253** (2007) 9061-9066. Doi: 10.1016/j.apsusc.2007.05.016
12. Y. Kayali, I. Gunes, S. Ulu, *Vacuum* **86** (2012) 1428-1434. Doi: 10.1016/j.vacuum.2012.03.030
13. Y. Kayali, B. Anaturk, *Mater. Des.* **46** (2013) 776-783. Doi: 10.1016/j.matdes.2012.11.040
14. A.A. Joshi, S.S. Hosmani, *Materials and Manufacturing Processes*, **29** (2014) 1062-1072. Doi: 10.1080/10426914.2014.921705
15. M. Keddam, R. Chegroune, *Appl. Surf. Sci.* **256** (2010) 5025-5030. Doi: 10.1016/j.apsusc.2010.03.048
16. S.A. Kusmanov, I.V. Tambovskiy, V.S. Sevostyanova, S.V. Savushkina, P.N. Belkin, *Surface and Coatings Technology*, **291** (2016) 334-341. Doi: 10.1016/j.surfcoat.2016.02.062
17. A. Piasecki, M. Kulka, M. Kotkowiak *Tribology International* **97** (2016) 173-191. Doi: 10.1016/j.triboint.2016.01.028
18. J.M. Johnston, M. Jubinsky, S.A. Catledge, *Applied Surface Science*, **328** (2015) 133-139. Doi: 10.1016/j.apsusc.2014.11.129
19. J. Zuno-Silva *et al.*, *J. Min. Metall. Select. B-Metall.*, **50** (2014) 101-107. Doi: 10.2298/JMMB140323019Z
20. N. Makuch, M. Kulka, *Fracture toughness of hard ceramic phases produced on Nimonic 80A-alloy by gas boriding, ceramics international* **42** (2016) 3275-3289.
21. O.I. Lomovsky, G.V. Golubkova, N.V. Bulina, I. Yadroitsev, I. Smurov, (2013); **49** 564-567. <http://dx.doi.org/10.1134/S002016851306006X>
22. M. Tabur, M. Izciler, F. Gul, I. Karacan, *Wear* **266** (2009) 1106-1112. Doi: 10.1016/j.wear.2009.03.006
23. B. Xiao, J.D. Xing, S.F. Ding, W. Su, *Physica B*, **403** (2008) 1723-1730. Doi: 10.1016/j.physb.2007.10.014
24. I. Gunes, S. Kanat, *Protection of Metals and Physical Chemistry of Surfaces*, **51** (2012) 842-846. Doi: 10.1134/S2070205115050111
25. O. Ozdemir, M. Usta, C. Bindal, A. Hikmet-Ucisik, *Hard iron boride (Fe<sub>2</sub>B) on 99.97 wt% pure iron*, *Vacuum*, **80** (2006) 1391-1395. Doi: 10.1016/j.vacuum.2006.01.022
26. I. Gunes, M. Erdogan, A. Gürhan-Çelik, *Materials Research*, **17** (2014) 612-618. Doi: 10.1590/S1516-14392014005000061
27. J. Jiang, Y. Wang, Q. Zhong, Q. Zhou, L. Zhang, *Surf. Coat. Technol.* **206** (2011) 473-478. Doi: 10.1016/j.surfcoat.2011.07.053
28. G.A. Baglyuk, A.A. Mamonova, C.G. Pyatachuk, L.A. Sosnovskii, *Powder Metall. Met. Ceram.*, **52** (2013) 113-117. Doi: 10.1007/s11106-013-9502-1
29. S. Sahin, C. Meric, *Mater. Res. Bull.* **37** (2012) 971-979. Doi: 10.1016/S0025-5408(02)00697-9
30. I. Gunes, *Kinetics of borided gear steels. Sadhana*, **38** (2013) 527-541. Doi: 10.1007/s12046-013-0138-0
31. B.D. Ratner, A.S. Hoffman, F.J. Schoen, J.E. Lemons, *Biomaterials Science: An Introduction to Materials in Medicine*, (Academic press; 2012), pp. 115.
32. Y. Bedolla-Gil, A. Juárez-Hernandez, A. Perez-Unzueta, E. Garcia-Sanchez, R. Mercado-Solís, M.A.L. Hernandez-Rodriguez, *Rev. Mex. Fis. S.*, **55** (2009) 1-5.
33. I. Campos-Silva *et al.*, *Surface & Coatings Technology*, **237** (2013) 402-414. Doi: 10.1016/j.surfcoat.2013.06.083
34. M. Dong, S. Bao-luo, Z. Xin, *Materials and Design*, **31** (2010) 3933-3936. Doi: 10.1016/j.matdes.2010.03.024
35. M. Dong, S. Bao-luo, *International Journal of Refractory Metals and Hard Materials*, **28** (2010) 424-428. Doi: 10.1016/j.ijrmhm.2010.01.003
36. A. Márquez-Herrera, J.L. Fernandez-Muñoz, M. Zapata-Torres, M. Melendez-Lira, P. Cruz-Alcantar, *Surface and Coatings Technology*, **254** (2014) 433-439. Doi: 10.1016/j.surfcoat.2014.07.001
37. A. Márquez-Herrera, G. Bermudez-Rodriguez, E.N. Hernandez-Rodriguez, M. Melendez-Lira, M. Zapata-Torres, *Int. J. Mater. Res. (formerly Z. Metallkd. E)*, **107** (2016) 1-3. Doi: 10.3139/146.111387
38. M.R. Shirdar *et al.*, *Ceramics International* **42** (2016) 6942-6954.
39. R. De-la-Vara-Salazar, H. Gutierrez-Pulido, *Análisis y diseño de experimentos*, 3 ed., (Mc. Graw Hill, México, 2012).
40. I. Campos-Silva *et al.*, *Surface & Coatings Technology* **260** (2014) 362-368. Doi: 10.1016/j.surfcoat.2014.07.092

41. G.A. Rodríguez-Castro *et al.*, *Surface & Coatings Technology*, **284** (2015) 258-263. Doi: 10.1016/j.surfcoat.2015.06.081
42. A.N. Minkevich, *Met. Sci. Heat Treat.* **3** (1961) 347-351. Doi: 10.1007/BF00810400
43. P.A. Dearnley, T. Bell, *Engineering the Surface with Boron Based Materials*, *Surf. Eng.* **1** (1985) 203-217. Doi: 10.1179/sur.1985.1.3.203
44. R. Ribeiro, S. Ingole, O. Juan, H. Liang, M. Usta, C. Bindal and A.H. Ucisik, *Tribological properties of boronized chromium for the biological applications*, *World Congress on Medical Physics and Biomedical Engineering*, **14** (2006) 3326-3330.
45. S. Okada, T. Atoda, I. Higashi and Y. Takahashi, *J. Mater. Sci.* **22** (1987) 2993-2999. Doi: 10.1007/BF01086503